Separation of Methylated Histone Peptides via Host-Assisted Capillary Electrophoresis

Jiwon Lee,[1] Lizeth Perez,[1] Yang Liu,[2] Hua Wang,[4,1] Richard J. Hooley,[1,3] and Wenwan Zhong[1,2*]

[1]Department of Chemistry; [2]Environmental Toxicology Program; [3]Department of Biochemistry and Molecular Biology; University of California-Riverside, Riverside, CA 92521, U.S.A. [4]Instrument Analysis Center, Yancheng Teachers University, Yancheng, Jiangsu 224007, China. E-mail: wenwan.zhong@ucr.edu, Fax: +1 951 827 4713.

ABSTRACT: Lysine methylation in protein is one important epigenetic mechanism that regulates diverse biological processes, but is challenging to study due to the large variability in methylation levels and sites. Here we show that supramolecular hosts such as calixarenes and cucurbiturils can be applied in the background electrolyte (BGE) of capillary electrophoresis (CE) for highly effective separation of post-translationally methylated histone peptides. The molecular recognition event causes a shift in the electrophoretic mobility of the peptide, allowing affinity measurement for binding between the synthetic receptor and various methylated lysine species. Successful separation of the H3 peptides carrying different methylation levels at the K9 position can be achieved using **CX4** and **CX6** as the BGE additives in CE, enabling monitoring of the activity of the histone lysine demethylase KDM6B. This reveals the power of combining high resolution CE with synthetic hosts for study of protein methylation, and the method should be capable of analyzing complex biological samples for better understanding of the functions of histone methylation.

Introduction

Post-translational modifications on proteins, including phosphorylation, acetylation, ubiquitination, and methylation, greatly expand the structural and function diversity of the proteome. PTMs impact almost all dynamic cellular processes, and monitoring PTM changes in biological systems is important in determining the regulation mechanisms of cellular signaling networks. Although great effort has been invested in improving PTM identification, it remains challenging due to their large variety in modification type and location.[1] While mass spectrometry is powerful for recognizing different modifications on peptides, prior separation is essential to reduce sample complexity and resolve modified proteins or peptides from the unmodified forms. Chromatographic methods, such as reversed-phase liquid chromatography (RPLC),[2] ion exchange chromatography (IEC), and hydrophilic interaction chromatography (HILIC),[3] have been developed for analyzing PTMs that effect distinguishable changes in charge, M_w, and hydrophobicity of the proteins or peptides. However, for PTMs that induce small overall changes, long separation times, multiple separation dimensions,[4] and extensive method optimization are typically required. An example of a common, yet challenging modification to detect is lysine methylation. Histone lysine modifications have been linked to gene activation and silencing, and they affect cell function, signaling pathways, playing important roles in disease development.[5,6] The modification occurs at different levels: mono-, di-, and tri-methylations can be found on different sites within histones, and occur at both lysine and arginine residues. Methylation does not change the overall charge of the residue, conferring only small changes in peptide size and hydrophobicity. Thus, discrimination between each methylation level and different methylation sites is challenging. More selective recognition of these modified side chains is required to improve the resolution of different types of PTMs and reduce the complexity in separation methods.

Antibodies are often used as the recognition units for peptide PTMs,[7,8] but they can be costly and time consuming to develop. Individual antibodies are often specific to only one type/state of modification,[9] and the selectivity can be reduced due to interference of neighboring PTMs.[10] Native receptors for PTMs have also been reported, such as the heterochromatin protein 1 (HP1) that can bind to methylated histone peptides with low dissociation constants.[11] These high affinity, high M_w binders are useful in PTM enrichment, but are not effective tools for column separation of diverse PTMs, because their high affinity significantly reduces column efficiency.

Synthetic receptors are attractive alternatives for PTM recognition, as they are more accessible than antibodies. Synthetic receptors such as cyclodextrins[12–14] and crown ethers[15] have been applied in chromatography and capillary electrophoresis (CE) for separation of chemically similar small molecules. CE is ideally suited to the application of synthetic receptors, as it only requires simple addition of the receptors to the separation media and different receptors can be easily employed. The high resolving power of CE can work in tandem with the recognition event, effecting improved PTM separation even if the receptor does not provide sufficient discrimination among targets with similar structures by itself. Here, we explore the possibility of using synthetic receptors to improve the separation by CE

of PTM peptide targets variably methylated at lysine residues (Figure 1a). Although CE has been used in the analysis of PTMs such as phosphorylation[16] and acetylation,[17] it has not yet been capable of separating methylated and non-methylated peptides in the absence of additives.

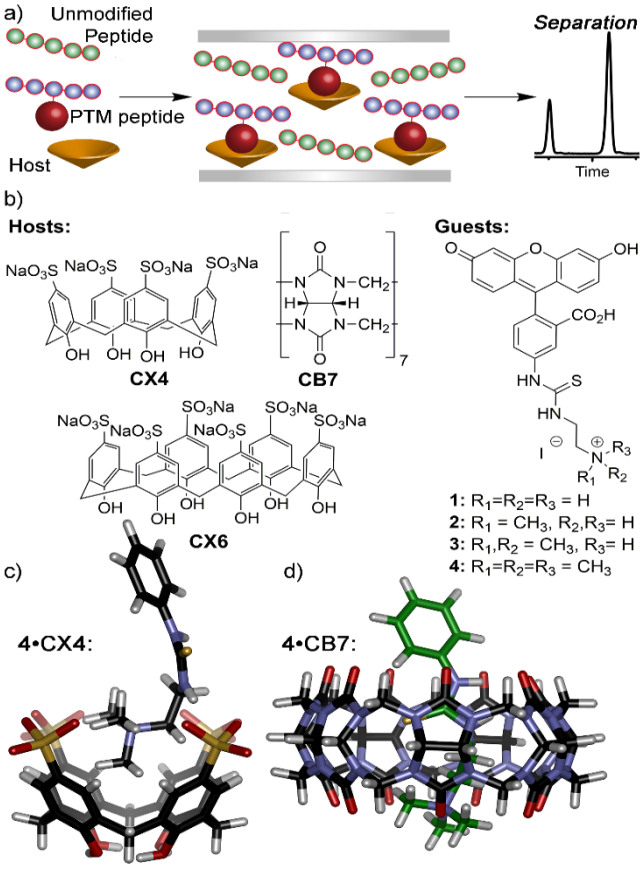

Figure 1. a) Representation of the host-assisted CE process. b) Structures of the hosts and guests used in this study; minimized structures of the c) **4•CX4** and **4•CB7** complexes, illustrating the host:guest interactions (SPARTAN, AM1 forcefield).

Synthetic receptors of various types are effective for the molecular recognition of methylation lysine residues. Examples include calixarenes,[18-22] cucurbiturils,[23-25] cyclophanes,[26-29] and deep cavitands.[30-32] The molecular recognition events are well-studied, and the receptors have been applied for selective sensing of histone modifications[31,33] as well as in supramolecular tandem assays.[32,34-37] However, the application of synthetic receptors to improve separation of methylated peptides from the unmethylated counterparts is rare, and often requires tethering of the host to the capillary.[22] Covalent attachment of the receptors to solid supports introduces synthetic challenges, and some hosts (especially cucurbiturils) are challenging to derivatize.[38] As CE only requires addition of the host to the running buffer, we were able to test simple, underivatized hosts for the process. We chose tetrasulfonatocalix[4]arene (**CX4**), hexasulfonatocalix[6]arene (**CX6**) and cucurbit[7]uril (**CB7**) in our study, because they are highly water-soluble and contain both a hydrophobic cavity with fixed size and an electron rich upper rim (Figure 1b). These hosts were capable of selective, varied molecular recognition of small molecule fluorophores and histone peptides in CE, and CE methods were developed for successful separation of methylated histone peptides that carry different methylation states and sites.

Materials and Methods

General. All samples and separation buffers were made using ultrapure water (18 MΩ) that was obtained from a Direct-Q Water Purification System (Millipore Sigma, Billerica, MA). Fluorophores **1-4** were synthesized according to literature procedures.[30,39] 4-Tetrasulfonatocalix[4]arene and cucurbit[7]uril hydrate were purchased from Sigma-Aldrich (St. Louis, MO). 4-Hexasulfonatocalix[6]arene hydrate was purchased from Alfa Aesar (Tewksbury, MA, USA). Lyophilized histone K27 peptides were purchased from AnaSpec, Inc. (Fremont, CA). The sequence is ARTKQTAR-K(me_x)-STGGKAPRKQLA (x = 0, 1, 2, 3). The peptide had either non-, mono-, di-, or trimethylation. Custom labeled nonmethylated and trimethylated histone K9 peptides were purchased from United Biochemical Research, Inc. (Seattle, WA). The sequence of each peptide is FITC-Ahx-AAR-K(me_x)-SAPY-COOH (x = 0 ,3).

Separation of small guests and fluorescently labeled H3K27 peptides. The CE experiments on the fluorescent guests were carried out using a homemade instrument equipped with a 488-nm excitation Argon Ion laser (Melles Griot Laser Group, Carlsbad, CA) for laser-induced fluorescence (LIF) detection. Separation power was provided by a TriSep 2100 HV voltage supplier (Unimicro Technologies, Pleasonton, CA). Bare fused-silica capillaries (50 µm i.d., 365 µm o.d.) were purchased from Polymicro Technologies (Phoenix, Arizona). The running buffer was 20 mM phosphate buffer, pH 7.4, with or without the synthetic hosts. The capillary was flushed prior to each separation with 0.1 M NaOH, ultrapure H_2O, and running buffer using a syringe pump. Samples were injected via gravity pressure. Electrophoresis was driven by an electric field of 250 V/cm with positive polarity. The effective length of the capillary was 45 cm. Electropherograms were acquired using PeakSimple Chromatography Software (SRI Instruments, Torrance, CA). Riboflavin was included as the internal standard for the small guest study. In the peptide study, fluorescein was used as an internal standard in CE-LIF.

Separation of methylated H3 peptides in a coated capillary. The separation of the non-fluorescently labeled, methylated peptides was performed in a polyvinyl alcohol (PVA)-coated capillary (50 µm inner diameter, 365 µm outer diameter) from Agilent Technologies (Santa Clara, CA). DMSO was included in the sample as an internal standard. Separation was conducted on an Agilent 7100 CE system with a UV absorption detector. Samples were introduced into the PVA capillary (50 µm inner diameter, 365 µm outer diameter, with an effective length of 35 cm) with a 50 mbar injection for 5s. Separation was driven by an electric field of 571 V/cm with positive polarity and 5 mbar of pressure. Prior to each day's experiment, the

capillary was flushed with 10 mM phosphoric acid and H_2O. Data was acquired via ChemStation (Agilent Technologies, Santa Clara, CA).

Lysine demethylation assay. The demethylation assay was performed using the custom labeled trimethylated peptide, FITC-Ahx-AAR-K(me_3)-SAPY-COOH, and human recombinant demethylase KDM6B (Reaction Biology Corp., Malvern, PA). Two μM of the FITC-labeled H3K27me_3 peptide was incubated with 1 μM KDM6B at room temperature in the reaction buffer (20 mM Tris-HCl, pH 7.4, 100 mM NaCl, 20 μM $(NH_4)_2Fe(SO_4)_2{\cdot}6(H_2O)$, 50 μM α-ketoglutaric acid, 500 μM ascorbate) with or without 1 μM 2,4-pyridinedicarboxylic acid (Cayman Chemical, Ann Arbor, Michigan). The reaction mixture was injected into the bare fused-silica capillary (50 μm inner diameter, 365 μm outer diameter) at time intervals between 0 and 9 hours. The running buffer was 50 μM **CX4** in 20 mM phosphate buffer, pH 7.4.

Mobility and affinity calculation. All mobilities in the following text are the electrophoretic mobility after EOF adjustment using the following equation:

$$\mu = \frac{L_t x\, L_d}{V}\left(\frac{1}{t_G} - \frac{1}{t_{IS}}\right) \qquad (1)$$

with L_t = total length of the capillary, L_d = length of the capillary from the inlet to the detection window, V = voltage, t_G = migration time of the guest, and t_{IS} = migration time of the internal standard. Binding constants were calculated as reported in affinity CE, using the Hill Equation (2), with n being the Hill coefficient for measurement of the guest's binding cooperativity:[40-42]

$$(\mu_i - \mu_0) = \frac{(\mu_{max} - \mu_0)[L]^n}{K_d + [L]^n} \qquad (2)$$

The percent change in mobility, %Δμ, was calculated for each host molecule via the following equation:

$$\%\Delta\mu = \frac{\mu_i - \mu_0}{\mu_0} \qquad (3)$$

with μ_o being the mobility without the host and μ_i being the mobility with the host at one concentration in the running buffer.

Results and Discussion

Analysis of binding with small guests. We initially determined the effectiveness of the three hosts in binding and separating small molecules that varied only in methylation state. Fluorophores **1-4** (Fig. 1b) were used as the model compounds to allow simple detection of the separation event: guests **1-4**[30,39] were synthesized in 2 or 3 steps from commercial materials, and the fluorescein label permitted LIF detection eliminating the problem of high background UV absorption with increasing host concentration in the background electrolyte (BGE) (Figure S1). The three host molecules, **CX4**, **CX6** and **CB7** are all capable of molecular recognition of substituted ammonium species, although their affinities and selectivities are somewhat different. The bowl-shaped, highly anionic **CX4** exploits charge matching cation-π interaction with the guest for maximal affinity. **CX6** has a larger cavity, but is far more flexible, whereas **CB7** is extremely rigid, and relies on a combination of hydrophobic interactions, London Dispersion forces and self-complementary hydrogen bonding at the upper rim to maximize selectivity.[19,23] Their selectivity for the various N-methylated states of lysine is limited, however, as the affinities for K, Kme_1, Kme_2 and Kme_3 are quite similar.[43-45] The best targets for **CB7** is N-terminal phenylalanine residues,[46-48] and functionalized derivatives of **CX4** are most effective at selective recognition of N-methylated lysines, rather than **CX4** itself.[18-22,33] **CX4** shows millimolar affinity for lysine at in buffered PBS at neutral pH,[49] as does **CB7**,[37,45] whereas the more flexible **CX6** favors larger substrates such as arginine, although the affinity for ammonium groups is ~10-fold less than that of **CX4**.[49]

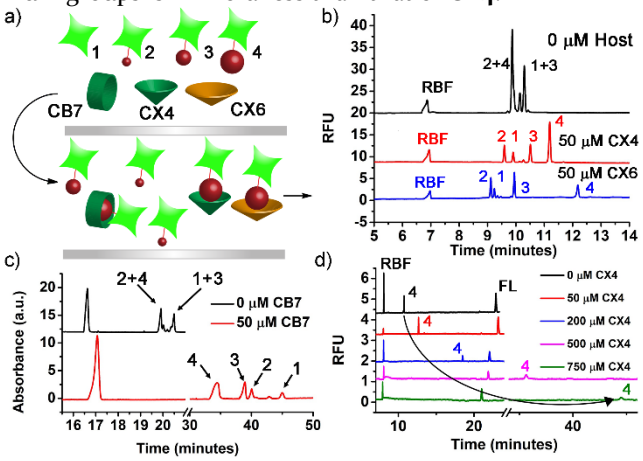

Figure 2. a) Small molecule separation via Host-Assisted CE. b) Separation of a small methylated guest mixture in 0 μM host vs. 50 μM **CX4** and **CX6.** [**1**] = 25 nM, [**2**] = 50 nM, [**3**] = 100 nM, [**4**] = 200 nM. c) Separation of a small methylated guest mixture in 0 μM vs. 50 μM **CB7** (detected by UV absorption detector). [**1**] = 50 μM, [**2**] = 100 μM, [**3**] = 200 μM, [**4**] = 500 μM. d) Mobility shift of the small trimethylated guest as more **CX4** is added to the BGE. RBF = 10 μM riboflavin, FL = 50 nM fluorescein, [**4**] = 50 nM.

To evaluate the binding between each host and the methylated guests, we employed affinity CE by putting the host in the BGE and monitored the migration of the guest (Figure 2a). Adding the hosts to the BGE may change the electroosmotic flow (EOF) by altering the charge density of the capillary wall (if the host is adsorbed onto the wall), as well as varying the viscosity of the BGE. Thus, the neutral dye riboflavin (RBF) was used as an internal standard (IS) to determine any changes in EOF. We also added a second IS, fluorescein (FL), to confirm that the label had no specific binding to the host. The resultant electropherograms with 50 μM host in the BGE are shown in Figures 2b,c. The guest molecules carry net negative charges at pH 7.4 as they all migrate later than the neutral marker. In the absence of host, **2** and **4** were not resolved at all, and neither were **1** and **3** (the small peak in between the two overlapped peaks was from impurity in the samples). The addition of **CX4** and **CX6** to the BGE caused the mobility for all methylated guests to become more negative (Table 1), due to the interaction between the guest and the multi-anionic hosts. The charge increase exceeds the increase in size, leading to an overall increase in the charge-to-size ratio. Interestingly, **CB7** in the BGE reduces the net mobility of each guest, presumably because the **CB7**-guest complex

has a larger hydration size than the guest itself but with no additional charges. The delay in the migration time of the neutral marker also implied a reduction in the EOF with an increase in [**CB7**]. We also tried to measure the binding affinity using the more conventional method of isothermal titration calorimetry (ITC). However, the small molecule-host binding released very small amounts of heat, making accurate measurement difficult. Still, for the binding between CX4 and guest **3** and **4**, the averaged K_d values obtained (157 μM and 125 μM for 3 and 4, respectively) were comparable to what measured by CE (Table S1). This comparison highlights the advantage of using CE for measurement of binding between small molecules and synthetic hosts.

Table 1: Mobility Changes and Dissociation Constants for Guest Fluorophores in the Hosts[a]

	Mobility Change, %			Guest Affinity	
Guest	**CX4**	**CX6**	**CB7**	Complex	K_d, μM
1	-6.4	1.8	5.7	**2**•**CX4**	299±30
2	9.8	-1.8	4.5	**3**•**CX4**	192±7
3	-9.2	-15.2	14.5	**4**•**CX4**	100±30
4	-26.0	-54.4	16.0	**4**•**CX6**	135±21
				4•**CB7**	51±4

[a] For mobility change (%), each host was kept at 50 μM for separation of the small guest mixture. With **CX4** or **CX6** in the BGE, [**1**] = 25 nM, [**2**] = 50 nM, [**3**] = 100 nM, [**4**] = 200 nM. With **CB7** in the BGE, [**1**] = 50 μM, [**2**] = 100 μM, [**3**] = 200 μM, [**4**] = 500 μM. BGE = Host in 20 mM sodium phosphate buffer, pH 7.4. Mobility change and guest affinity results are averages of 2-3 replicate measurements. Hill coefficient and fitting R^2 were reported in Table S1 in Supporting Information.

The elution order of the four small guests is dependent on their relative affinity to the host in the BGE. The guest that binds to the host with the highest affinity should exhibit the largest change in mobility. For all hosts, the trimethylated guest **4** exhibited the largest mobility shift among the guest molecules, indicating the strongest affinity to the hosts. To find the binding affinity, the mobility shifts (Δμ) of the methylated guest induced by varying host concentrations in the BGE were measured (Figure 2d and Figure S2 – S6), and plotted vs. [host]. The resultant binding curves were fit with equation (2) to allow calculation of dissociation constant K_d for the host:guest complexes (Table 1, Figure S2-S6). The non-methylated guest **1** did not show a consistent change in its mobility with any of the host, indicating no binding, thus no K_d was obtained. There is a two-fold variation in affinity between guests **2-4** in **CX4**: the greater the methylation level of the guest, the stronger the affinity for the host, which is consistent with other binding affinity studies.[50-52] While the affinity of **4** with **CX4** increased by one fold compared to that of **3**, the difference in the K_d values between **3** and **2** is smaller, about 50%. Addition of the third methyl group significantly enhances the binding between the methylated lysine guests and the receptors. Higher resolution separation of **4** from **3** or **2** was possible than for the guests with lower methylation levels. The affinities of the trimethylated fluorophore **4** vary between the different hosts. The more flexible **CX6** displays a lower affinity for **4**, whereas the more effective host **CB7** binds **4** most strongly (K_d = 51 ± 4 μM), consistent with literature reports for similar species.[23]

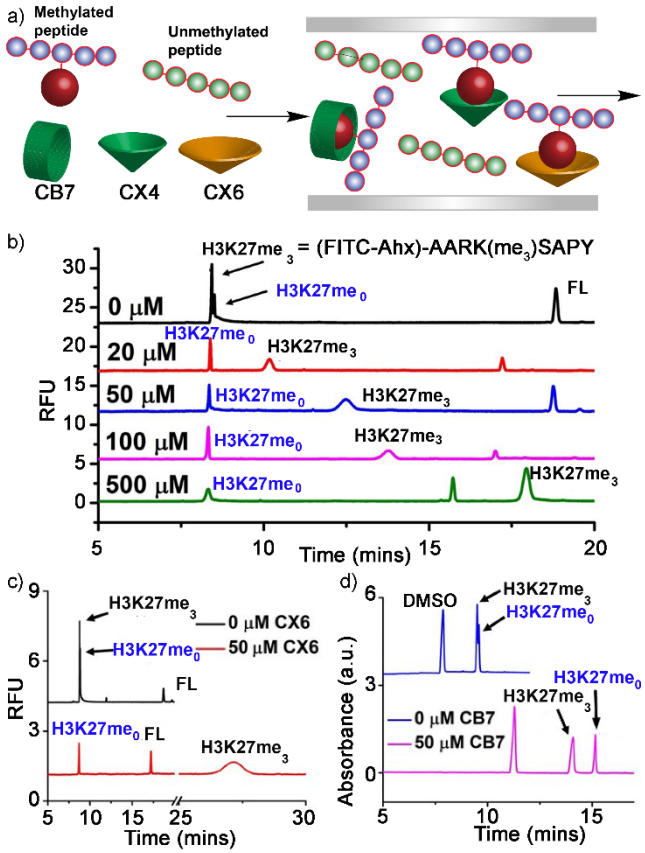

Figure 3. a) Methylated peptide separation via Host-Assisted CE. Mobility shift of the labeled $H3K27me_3$ peptide with increasing b) [**CX4**], c) [**CX6**] and d) [**CB7**]. FL = fluorescein as the internal standard. The sequences of the H3K27 peptides are (FITC-Ahx)-AARK($me_{0/3}$)SAPY. [peptide] = 0.5 μM.

Analysis of binding with trimethylated peptides. The differential binding and separation of the control fluorophores with varying methylation states at N is encouraging, and indicates the potential of host-assisted CE for the separation of variably methylated histone peptides. We next analyzed the binding between the four hosts and a trimethylated Histone H3K27 peptide (Figure 3a). A fluorescent $H3K27(me_3)$ peptide, N-terminally labeled with fluorescein and an aminohexanoate spacer (FITC-Ahx) was used as target to allow LIF detection, minimizing the background signal from the hosts in BGE. The unmethylated H3K27 peptide equivalent ($H3Kme_o$) was used as a control. Both cationic peptides migrated faster in the BGE than the anionic fluorescein internal standard. In the absence of any host, the two peptides (0.5 μM) were barely separated (Figure 3b). Increasing **CX4** concentration in the BGE extended the migration time of the trimethylated peptide significantly, while the mobility of the unmethylated peptide was essentially unchanged. The mobility change of labeled $H3K27(me_3)$ is 64%, with [CX4] = 50 μM, which is more

than two times of the 26% decrease of **4** in **CX4**. The resolution (R) value between the H3K27(me_0) and H3K27(me_3) was as large as 4.4 at this host concentration (Table S3). Plotting the mobility shift curve against the host concentration and fitting to equation (2) showed that the affinity of the H3K27(me_3) peptide was higher than that of **4**, with K_d = 48 ± 7 μM (Table 2). In contrast, the nonmethylated H3K27 peptide did not exhibit a sigmoidal relationship between the mobility shift and host concentration, indicating no affinity with **CX4** (Figure S7).

The other hosts were even more effective at binding the H3K27(me_3) peptide, as shown in Table 2. **CB7** was the strongest host, with K_d = 5.5 ± 0.7 μM, and **CX6** was a better host than **CX4**, with K_d = 17.7 ± 4.2 μM (Figure S8). Interestingly, the migration order between H3K27(me_3) and H3K27 varied with the type of guest. Both of the sulfonated calixarene hosts are anionic, causing the calixarene-peptide complex to have a more negative electrophoretic mobility than the free peptide, and migrate slower. In contrast, the neutral cucurbituril effects an increase in overall size upon binding with no global change in charge difference, resulting in a less negative electrophoretic mobility and a faster elution time for the host-peptide complex. However, **CB7** can adsorb to the silica wall and reduce the EOF. With high concentrations (>100 μM) of **CB7** in the BGE (Figure S9), the EOF drops significantly and increases the elution time for all analytes, which contributes to peak broadening, lowering the column efficiency. The anionic calixarenes do not adhere to the anionic silica wall, and as such effect minimal EOF change even at high concentrations. Again, the affinity values reported in Table 2 were confirmed by ITC measurement (Table S2, Supporting Information), which consumed much more peptides than the CE method.

Table 2: Dissociation constants of labeled H3K27(me_3) when bound to the various hosts.[a]

Host	K_d, μM	n	R^2
CX4	48.0 ± 7.0	1.3	0.995
CX6	17.7 ± 4.2	1.4	0.999
CB7	5.5 ± 0.7	1.0	0.956

[a][H3K27(me_3)] = 0.5 μM in **CX4** and **CX6** BGE. 100 μM H3K27(me_3) in **CB7** BGE. Host in 20 mM sodium phosphate buffer, pH 7.4. Results are averages of triplicate measurements.

Separation of peptides with different methylation levels. The host-assisted CE process was highly effective for separation of trimethylated and unmethylated peptides. The more challenging and desirable task is to separate PTM peptides with only slightly different methylation states (i.e. 0, 1, 2 and 3) (Figure 4a). We extended the separation process to four peptides based on the H3K9me sequence, with no N-terminal fluorophore and varying K9 methylation levels (0-3), which were more representative of the peptides accessible from biological samples than the fluorescently labeled peptides used previously. These peptides were larger than the K27 counterparts, consisting of 21 amino acid residues with a M_w ~ 2.2 - 2.3 kDa and a pI of 12.14. These longer peptides are more basic, and as such, a polyvinyl alcohol (PVA) coated capillary was employed to prevent adsorption of the highly cationic peptides.[17, 53,54] Since the EOF was almost zero in this coated capillary, hydrodynamic pressure (5 mbar), was applied in addition to the electric field to ensure reasonable separation times for the peptide-host complex.

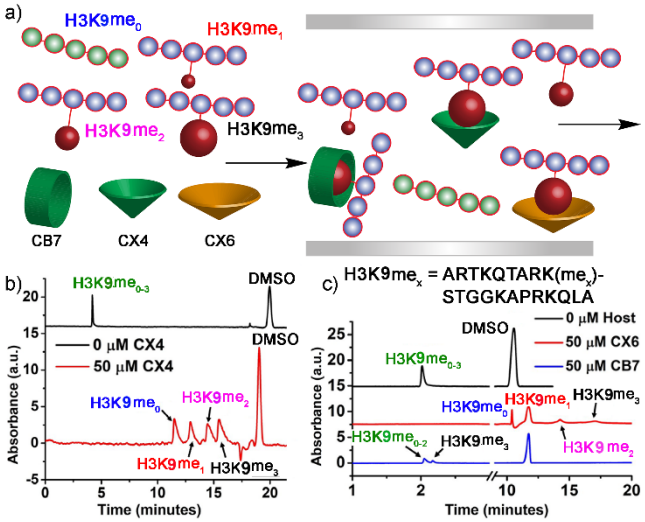

Figure 4. a) Separation of H3K9 peptides with varying methylation levels. b) Mobility shifts of the labeled H3K9me_{0-3} peptide mixture with increasing [CX4]; c) Mobility shifts of the labeled H3K9me_{0-3} peptide mixture with increasing [CX6] and [CB7]. 0.1% DMSO as internal standard, [peptide] = 50 μM.

As shown in Figure 4b and c, all four K9 peptides ([peptide] = 50 μM) show identical mobilities in the absence of any host in the BGE. Since the K9 peptides are larger in size, a M_w difference of 14 Da does not induce sufficient change in the electrophoretic mobility between different methylation levels for effective separation. In the presence of 50 μM **CX4** in the BGE, all four peptides could be efficiently separated (Figure 4b), with longer elution times being observed as the methylation state increases: H3K9me_0 eluted first, and H3K9me_3 last, indicating increased affinity of the higher methylation states to the host. Identity of each peak was confirmed by spiking the individual peptide to the mixture and observing increase in the peak area (Supporting Information, Figure S10). The resolution between H3K9me_0 and H3K9me_1 was better than that between H3K9me_2 and H3K9me_3 (Table 3). **CX4** absorbs at 214 nm, thus a relatively higher peptide concentration of 100 μM was injected here (compared to 0.5 μM in the separation with the LIF detector) to overcome background signal. Each peptide peak displayed a sharp front and a tailing end, which is induced by the mobility difference between the peptide and the host-peptide complex. For peptides that diffuse out of the sample zone at the front boundary, binding to the host in the BGE slowed down their migration, and thus the peptide is pushed back to the sample zone, forming a sharp peak front. For the peptide diffusing out at the back boundary, binding slowed it down, leading to peak tailing.

Table 3: Resolution of the H3K9(me$_{0-3}$) peptides in the presence of hosts.[a]

Peptide Peaks	CX4	CX6	CB7
H3K9me$_0$/me$_1$	1.88	2.83	0
H3K9me$_1$/me$_2$	1.72	2.42	0
H3K9me$_2$/me$_3$	1.06	1.85	0.72

[a] 100 μM H3K9(me$_{0-3}$) injected into 20 mM sodium phosphate buffer, pH 7.4, [host] = 50 μM. Results are averages of duplicate measurements. See equation S2 for resolution definition.

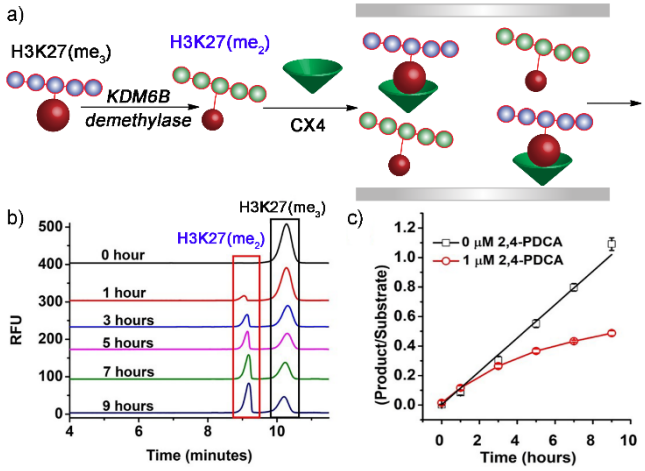

Figure 5. a) Host-assisted CE as a KDM6B demethylase assay. b) Separation of demethylated product H3K27(me$_2$) and H3K27(me$_3$) substrate after enzyme reaction for various times. c) Inhibitor assay: [H3K27(me$_2$)]/[H3K27(me$_3$)] versus time in the presence and absence of 1 μM 2,4-PDCA inhibitor, electropherograms shown in Figure S10.

We also evaluated separation with the other two hosts, keeping the peptide and host concentrations at 50 μM, and separated under the same hydrodynamic pressure of 5 mbar and an electric field of 571 V/cm. **CX6** effected the same migration order of the four H3K9(me$_{0-3}$) peptides as did **CX4**, but with better resolution (Figure 4c, Table 3). The broad peak for H3K9(me$_1$) is large due to overlap with the neutral marker. In contrast, **CB7** was a less effective additive, and only the trimethylated peptide H3K9(me$_3$) was separated from the mixture (Figure 4c), and even then, with a lower resolution of 0.72 (Table 3). This is unfortunate, as **CB7** is ideally suited to UV detection due to its minimal absorbance at 214nm. As such, there are no background issues even if high host concentrations are added to the BGE.

The good separation with **CX4** and **CX6** is mainly due to charge changes upon binding. As the H3K9(me$_{0-3}$) peptides are larger than the control fluorophores and H3K27 peptides, the change in overall size upon binding with the hosts is relatively small. In the case of **CB7**, which only effects a change in size and not charge, the host had less impact on peptide mobility upon binding, and, at 50 μM, it could not resolve the peptides with lower methylation levels.

Enzyme assay. As the host-assisted CE method could effectively separate peptides of varying methylation level, it is a valuable tool for studying the function of methylation-related enzymes and screening enzyme effectors or inhibitors. To demonstrate this, we applied the CE method to evaluate the activity of KDM6B, a demethylase selective for methylated H3K27 peptides (Figure 5a). This enzyme reduces the trimethylated H3K27 peptide to the demethylated, monomethylated and unmethylated states[55] in the presence of α-ketoglutarate and Fe^{2+} cofactors. Figure 5b shows the assay process for the demethylation of 2 μM H3K27(me$_3$) with 1 μM KDM6B, 50 μM α-ketoglutarate, 500 μM ascorbate, and 20 μM Fe^{2+} in 20 mM tris buffer, pH 7.4. Aliquots were extracted at hourly time points, and subjected to host-assisted CE, with 50 μM **CX4** in the BGE. Fluorescence monitoring prevents interference from the other reaction components, and can unambiguously detect the peptide substrate and the corresponding products. As time increased, the H3K27(me$_3$) substrate was consumed and a single product appeared (Fig. 5b). MALDI-MS analysis revealed that this product was the dimethylated species H3K27(me$_2$) (Figure S11). This demethylase seemed not particularly efficient: a reaction time longer than 5 hours led to only 20% turnover ratio, and only the dimethylated product was produced. Nevertheless, we could use this method to analyze the effect of a demethylase inhibitor, 2,4-pyridinedicarboxylic acid (2,4-PDCA), which is an inhibitor for several JmjC domain-containing enzymes. It targets the active site for iron on α-ketoglutarate, one of the cofactors important in demethylation.[55] Starting at the 3 hour data point, the area ratio of product to substrate decreased with the presence of 2,4-PDCA, indicating reduction of enzyme activity under the action of the inhibitor (Figure 5c and Table 4).

To prove that our method can also monitor reactions on unlabeled peptides, we applied it to evaluate the demethylation reaction catalyzed by JMJD2E on the not-fluorescently labeled H3K9me$_3$ as that used in Fig. 4. The non-label substrate would be more representative to the peptides obtained from biological samples, and it allows us to spike in standard peptides to confirm the identities of the product peaks. A higher substrate concentration of 50 μM was needed to permit UV detection, along with higher enzyme (5 μM JMJD2E) and co-factor concentrations (500 μM α-ketoglutarate, 5 mM ascorbate, and 100 μM Fe^{2+}). CE analysis was carried out at the discrete reaction time points of 0, 20, 60, and 120 min, with 50 μM **CX4** in the BGE. The electropherograms measured at λ_{abs} = 214 nm showed that the peak of H3K9(me$_3$) decreased dramatically at 20 min, with the appearance of some unresolved product peaks in the region where the peptides with lower methylation levels should locate (Supporting information, Fig. S13a). As the reaction went on, the products became better resolved: a clear product peak was observed at reaction duration of 60 min, which decreased with the next 60-min reaction and produced another peak at earlier elution time. Spiking the standard peptides of H3K9(me$_{0-3}$) to the reaction mixture obtained at 120 min helped to confirm the identity of each peak (Fig. S13b). The changes occurred in the reaction were also confirmed by MALDI-MS (Fig. S13c). With the

addition of 2,4-PDCA, obvious inhibition of the enzyme activity took place and no product generation was observed at reaction duration of either 20 or 60 min (Fig. S13d). It is interesting to notice that the electropherograms obtained at 20-min reaction duration had one additional peak showing up after adding the enzyme to the reaction mixture, which disappeared if the inhibitor was added (Fig. S13d). This peak may indicate the complex formed between the enzyme and the peptide substrate which was disrupted by the addition of 2,4-PDCA. More investigation should be performed on the enzyme reaction to reveal the full power of our method in functional study of methylation enzymes.

Table 4: Effect of demethylase inhibitor 2,4-PDCA on the demethylation reaction, monitored by host-assisted CE.

Time, h	Product Ratio, 0 μM PDCA[b]	Product Ratio, 1 μM PDCA[b]
0	0.003 ± 0.002	0.014± 0.016
1	0.085 ± 0.017	0.116 ± 0.016
3	0.304 ± 0.026	0.264 ± 0.016
5	0.552 ± 0.026	0.366 ± 0.015
7	0.797 ± 0.025	0.433 ± 0.007
9	1.091 ± 0.043	0.487 ± 0.018

[a] 2 μM H3K27(me_3) incubated with 1 M μKDM6B, 50 μM α-ketoglutarate, 500 μM ascorbate, and 20 μM Fe^{2+} in 20 mM tris buffer, pH 7.4, 100 mM NaCl. Results are averages of duplicate measurements. Electropherograms shown in Figure S12, Supporting Information.

The above results support that our method is capable of monitoring enzyme reactions and assessing enzyme activities with either the fluorescently labeled peptides or native peptides. Fluorescence detection is preferred because the peptides (both substrate and products) could be detected unambiguously without interference from other components in the reaction mixture.

Conclusions

Here, we have shown that capillary electrophoresis is an effective method of separating post-translationally modified histone peptides with only small variations in structure, when combined with a suitable host molecule in the background electrolyte. Even for large, 21-amino acid peptide substrates, the small physical change induced by the addition of only one methyl group to a single lysine residue can be separated. Selective molecular recognition events between calixarene and cucurbituril hosts confer varying changes in size and charge to the peptides. The combination of both molecular recognition and CE magnifies the efficiency of both techniques, allowing high separation efficiency, despite the minimal changes in peptide structure upon modification. Host-assisted CE is fast and consumes a minimal amount of reagents and samples. It is also versatile, as changing the separation medium is simple, and a library of hosts can be applied with no need for covalent attachment to capillary wall surfaces. All these features make host-assisted CE an ideal tool for separation and purification of modified peptides that are challenging to isolate with conventional methods. The host-assisted CE method can also be applied to monitor enzyme reactivity, which is advantageous due to the small sample consumption of CE, and continuous sampling which saves on samples and time. Future work in our laboratories will focus on coupling the host-assisted CE with MS to permit analysis of methylated peptides in more complex mixtures. Examination of protein methylation can then be carried out in biological samples such as cells and tissues for better understanding of the functions of these PTMs.

ASSOCIATED CONTENT

Supporting Information

Additional experimental details; absorbance spectra of the synthetic receptors; analysis of affinity between the synthetic hosts and the small guests, and the methylated peptides, summary of resolution in host-assisted CE, and results from the lysine demethylase assay. This material is available free of charge via the Internet at http://pubs.acs.org.

AUTHOR INFORMATION

Corresponding Authors

* Phone: +1 951 827 4925. Fax: +1 951 827 4713.
E-mail: wenwan.zhong@ucr.edu

ACKNOWLEDGMENTS

The authors would like to thank the National Science Foundation (CHE-1748063 to W.Z. and R.J.H.) for the support; and are grateful to Dr. Jikui Song and Mr. Linggeng Gao for their help with ITC measurement.

REFERENCES

(1) Olsen, J. V.; Mann, M. *Mol.Cell. Proteomics* **2013**, *12*, 3444-3452.
(2) Zhang, J.; Corbett, J. R.; Plymire, D. A.; Greenberg, B. M.; Patrie, S. M. *Proteomics* **2014**, *14*, 1223-1231.
(3) Zybailov, B.; Sun, Q.; van Wijk, K. J. *Anal. Chem.* **2009**, *81*, 8015-8024.
(4) Colignon, B.; Raes, M.; Dieu, M.; Delaive, E.; Mauro, S. *Proteomics* **2013**, *13*, 2077-2082.
(5) Anderton, J.A.; Bose, S.; Vockerodt, M.; Vrzalikova, K.; Wei, W.; Kuo, M.; Helin, K.; Christensen, J.; Rowe, M.; Murray, P.G.; Woodman, C.B. *Oncogene* **2011**, *30*, 2037-2043.
(6) Hua, K.T.; Wang, M.Y.; Chen, M.W.; Wei, L.H.; Chen, C.K.; Ko, C.H.; Jeng, Y.M.; Sung, P.L.; Jan, Y.H.; Hsiao, M.; Kuo, M.L.; Yen, M.L. *Mol. Cancer* **2014**, *13*, 1-13.
(7) Guo, A.; Gu, H.; Zhou, J.; Mulhern, D.; Wang, Y.; Lee, K.A.; Yang, V.; Aguiar, M.; Kornhauser, J.; Jia, X.; Ren, J.; Beausoleil, S.A.; Silva, J.C.; Vemulapalli, V.; Bedford, M.T.; Comb, M.J. *Mol. Cell. Proteomics* **2013**, *13*, 372-387.
(8) Garnett, G.A.E.; Starke, M.J.; Shaurya, A.; Li, J.; Hof, F. *Anal. Chem.* **2016**, *88*, 3697-3703.
(9) Santos-Rosa, H.; Schneider, R.; Bannister, A.J.; Sherriff, J.; Bernstein, B.E.; Tolga Emre, N.C.; Schreiber, S.L.; Mellor, J.; Kouzarides, T. *Nature* **2002**, *419*, 407-411.
(10) Rothbart, S.B.; Dickson, B.M.; Raab, J.R.; Grzybowski, A.T.; Krajewski, K.; Guo, A.H.; Shanle, E.K.; Josefowicz, S.Z.;

Fuchs, S.M.; Allis, C.D.; Magnuson, T.R.; Rutherburg, A.J.; Strahl, B.D. *Mol. Cell* **2015**, *59*, 502-511.
(11) Nielsen, P.R.; Nietlispach, D.; Mott, H.R.; Callaghan, J.; Bannister, A.; Kouzarides, T.; Murzin, A.G.; Murzina, N.V.; Laue, E.D. *Nature* **2002**, *416*, 103-107.
(12) Gong, Y.; Lee, H. K. *Anal. Chem.* **2003**, *75*, 1348-1354.
(13) Wu, S.-H.; Ding, W.-H. *Electrophoresis* **2005**, *26*, 3528-3537.
(14) Mitchell, C. R.; Armstrong, D. W. *Methods in Molecular Biology* **2004**, *243*, 61-112.
(15) Jin, Y.; Hirose, K.; Nakamura, T.; Nishioka, R.; Ueshige, T.; Tobe, Y. *J. Chromatogr. A* **2006**, *1129*, 201-207.
(16) Lindner, H.; Helliger, W.; Dirschlmayer, A.; Talasz, H.; Wurm, M.; Sarg, B.; Jaquemar, M.; Puschendorf, B. *J. Chromatogr.* **1992**, *608*, 211-216.
(17) Lindner, H.; Helliger, W.; Dirschlmayer, A.; Jaquemar, M.; Puschendorf, B. *Biochem. J.* **1992**, *283*, 467-471.
(18) Beshara, C.S.; Jones, C.E.; Daze, K.D.; Ligert, B.J.; Hof, F. *Chem. Bio. Chem.* **2010**, *11*, 63- 66.
(19) Daze, K.D.; Hof, F. *Acc. Chem. Res.*, **2013**, *46*, 937-945
(20) Hof, F. *Chem. Commun*. **2016**, 52, 10093-10108.
(21) Daze, K.D.; Pinter, T.; Beshara, C.S.; Ibraheem, A.; Minaker, S.A.; Ma, M.C.; Courtemanche, R.J.; Campbell, R.E.; Hof, F. *Chem. Sci.* **2012**, 3, 2695–2699.
(22) Garnett, G.A.E.; Starke, M.J.; Shaurya, A.; Li, J.; Hof, F. *Anal. Chem.* **2016**, *88*, 3697-3703.
(23) Barrow, S.J.; Kasera, S.; Rowland, M.J.; del Barrio, J.; Scherman, O.A. *Chem. Rev.* **2015**, *115*, 12320-12406.
(24) Assaf, K.I.; Nau, W.M. *Chem. Soc. Rev.* **2015**, *44*, 394-418.
(25) Mona A. Gamal-Eldin, M. A.; Macartney, D. H. *Org. Biomol. Chem.,* **2013**, *11, 488-495*.
(26) Ingerman, L. A.; Cuellar, M. E.; Waters, M. L. *Chem. Commun.* **2010**, *46*, 1839-1841.
(27) Pinkin, N. K.; Waters, M. L. *Org. Biomol. Chem.* **2014**, *12*, 7059-7067.
(28) James, L. I.; Beaver, J. E.; Rice, N. W.; Waters, M. L. *J. Am. Chem. Soc.* **2013**, *135*, 6450–6455.
(29) Gober, I. N.; Waters, M. L. *J. Am. Chem. Soc.* **2016**, *138*, 9452–9459.
(30) Liu, Y.; Perez, L.; Mettry, M.; Easley, C.J.; Hooley, R.J.; Zhong, W. *J. Am. Chem. Soc.* **2016**, *138*, 10746–10749.
(31) Liu, Y.; Perez, L.; Mettry, M.; Gill, A.D.; Byers, S. R.; Easley, C.J.; Bardeen, C.J.; Zhong, W.; Hooley, R.J. *Chem. Sci.* **2017**, *8*, 3960 - 3970.
(32) Liu, Y.; Perez, L.; Gill, A.D.; Mettry, M.; Li, L.; Wang, Y.; Hooley, R.J.; Zhong, W. *J. Am. Chem. Soc.* **2017**, *139*, 10964-10967.
(33) Minaker, S.A.; Daze, K.D.; Ma, M.C.F.; Hof, F. *J. Am. Chem. Soc.* **2012**, *134*, 11674–11680.
(34) Florea, M.; Kudithipudi, S.; Rei, A.; González-Álvarez, M. J.; Jeltsch, A.; Nau, W. M. *Chem.-Eur. J.* **2012**, *18*, 3521-3528.
(35) Peacor, B. C.; Ramsay, C. M.; Waters, M. L. *Chem. Sci.* **2017**, *8*, 1422-1428.
(36) Praetorius, A.; Bailey, D. M.; Schwarzlose, T.; Nau, W. M. *Org. Lett.* **2008**, 10, 4089-4092.
(37) Nau, W. M.; Ghale, G.; Hennig, A.; Bakirci, H.; Bailey, D. M. *J. Am. Chem. Soc.* **2009**, *131*, 11558-11570.
(38) Lucas, D.; Minami, T.; Iannuzzi, G.; Cao, L.; Wittenberg, J. B.; Anzenbacher, P., Jr.; Isaacs, L. *J. Am. Chem. Soc.* **2011**, *133*, 17966-17976.
(39) Liu, Y.; Liao, P.; Cheng, Q.; Hooley, R.J. *J. Am. Chem. Soc.* **2010**,*132*, 10383-10390.
(40) Rundlett, K. L.; Armstrong, D. W. *Electrophoresis* **2001**, *22*, 1419-1427.
(41) Chen, Z.; Weber, S. G. Tr. Anal. Chem. **2008**, 27, 738-748.
(42) Colquhoun, D. *Tr. Pharmacol. Sci.* 2006, 27, 149-157.
(43) McGovern, R.E.; Fernandes, H.; Khan, A.R.; Power, N.P.; Crowley, P.B. *Nat. Chem.* **2012**, *4*, 527-533.
(44) McGovern, R. E.; Snarr, B. D.; Lyons, J. A.; McFarlane, J.; Whiting, A. L.; Paci, I.; Hof, F.; Crowley, P. B. *Chem. Sci.* **2015**, *6*, 442-449.
(45) Bailey, D.M.; Hennig, A.; Uzunova, A.D.; Nau, W.M. *Chem. Eur. J.* **2008**, *14*, 6069 – 6077.
(46) Li, W.; Bockus, A.T.; Vinciguerra, B.; Isaacs, L.; Urbach, A.R. *Chem. Commun.* **2016**, 52, 8537-8540.
(47) Lee, J.W.; Lee, H.H.L.; Ko, Y.H.; Kim, K.; Kim, H.L. *J. Phys. Chem. B*, **2015**, *119*, 4628–4636.
(48) Lee, J.W.; Shin, M.H.; Mobley, W.; Urbach, A.R.; Kim, H.L. *J. Am. Chem. Soc.* **2015**, *137*, 15322–15329.
(49) Douteau-Guével, N.; Coleman, A.W.; Morel, J.-P.; Morel-Desrosiers, N. *J. Chem. Soc., Perkin Trans. 2*, **1999**, 629–633
(50) Nielsen, P.R.; Nietlispach, D.; Mott, H.R.; Callaghan, J.; Bannister, A.; Kouzarides, T.; Murzin, A.G.; Murzina, N.V.; Laue, E.D. *Nature* **2002**, *416*, 103-107.
(51) Hughes, R.M.; Wiggins, K.R.; Khorasanizadeh, S.; Waters, M.L. *Proc. Natl. Acad. Sci.* **2007**, *104*, 11184-11188.
(52) Taverna, S.D.; Li, H.; Ruthenburg, A.J.; Allis, C.D.; Patel, D.J. *Nat. Struct. Mol. Biol.* **2007**, *14*, 1025-1040.
(53) Horvath, J.; Dolnik, V. *Electrophoresis* **2001**, *22*, 644-655.
(54) Belder, D.; Deege, A.; Husmann, H.; Kohler, F.; Ludwig, M. *Electrophoresis* **2001**, *22*, 3813-3818.
(55) Rose, N.R.; McDonough, M.A.; King, O.N.F.; Kawamura, A.; Schofield, C.J. *Chem. Soc. Rev.* **2011**, *40*, 4364-4397.

For TOC Only:

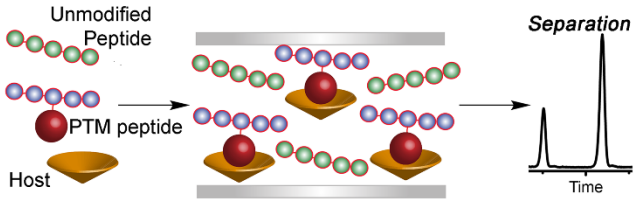

Supporting Information

Separation of Methylated Histone Peptides via Host-Assisted Capillary Electrophoresis

Jiwon Lee,[1] Lizeth Perez,[1] Yang Liu,[2] Hua Wang,[4,1] Richard J. Hooley,[1,3] and Wenwan Zhong[1,2*]

[1]Department of Chemistry; [2]Environmental Toxicology Program; [3]Department of Biochemistry and Molecular Biology; University of California-Riverside, Riverside, CA 92521, U.S.A.
[4]Instrument Analysis Center, Yancheng Teachers University, Yancheng, Jiangsu 224007, China

[*]Corresponding author:
E-mail: wenwan.zhong@ucr.edu
Fax: +1 951 827 4713.

Table of contents:

1. Additional Experimental Details

General. UV/vis spectra were obtained with a Varian, Inc. Cary 50 UV-Vis Spectrophotometer from Agilent Technologies (Santa Clara, CA, USA). The absorbance of 3 μM host solutions were measured in a Quartz Spectrophotometer Cell (100 μL, 10 mm, Z = 15 mm) from Starna Cells, Inc. (Atascadero, CA, USA).

The demethylation assay was performed using a H3K27me$_3$ (23-34) histone peptide purchased from AnaSpec, Inc. (Fremont, CA, USA). The peptide has the sequence, KAAR-K(Me$_3$)-SAPATGG. Human recombinant demethylase KDM6B was purchased from Reaction Biology Corp., Malvern, PA, USA). 4 μM H3K27me$_3$ peptide was incubated with 1.6 μM KDM6B at room temperature in the reaction buffer (50 mM Tris-HCl, pH 7.4, 100 mM NaCl, 6 μM $(NH_4)_2Fe(SO_4)_2 \cdot 6(H_2O)$, 50 μM α-ketoglutaric acid, 500 μM ascorbate). The reaction mixture was quenched with formic acid (final, 0.1%). MALDI spectra were obtained with a TOF/TOF 5800 System from AB Sciex (Framingham, MA, USA) on a 96-well MALDI plate insert.

Calculations. The K_d was calculated via the equation:

$$\Delta\mu = \frac{\Delta\mu_{max}[\boldsymbol{CX4}]^n}{{K_d}^n + [\boldsymbol{CX4}]^n} \qquad \text{(S1)}$$

where Δμ, mobility shift = $\mu_i - \mu_0$, n = binding coefficient, $\Delta\mu_{max}$ is the maximum mobility shift.

The resolution of two adjacent peaks was calculated with the equation:

$$R = \frac{t_1 - t_2}{\frac{1}{2}(w_1 + w_2)} \qquad \text{(S2)}$$

where t_1 = time of peak 1, t_2 = time of peak 2, w_1 = width of peak 1, and w_2 = width of peak 2.

2. Absorbance Spectra of Synthetic Hosts

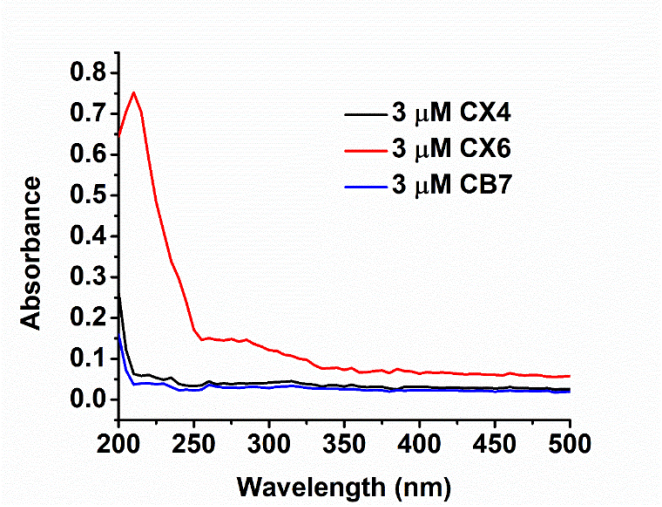

Figure S1. Absorbance spectra of 3 μM **CX4**, **CX6**, and **CB7** in water.

3. Analysis of Affinity between Small Guests and Synthetic Hosts

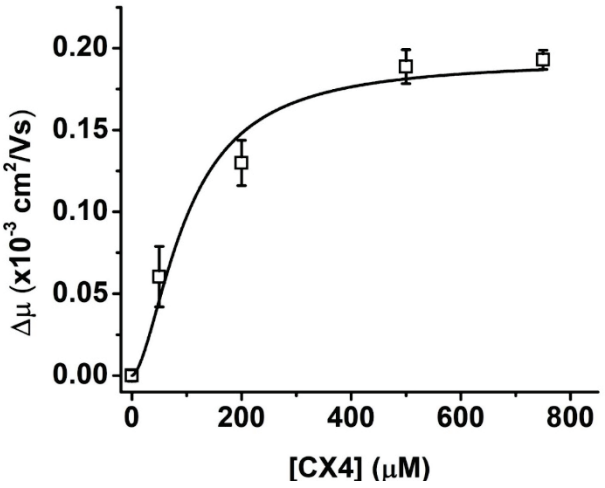

Figure S2. A plot of Δμ vs. [**CX4**] for guest **4**. Each data point consists of triplicate measurements.

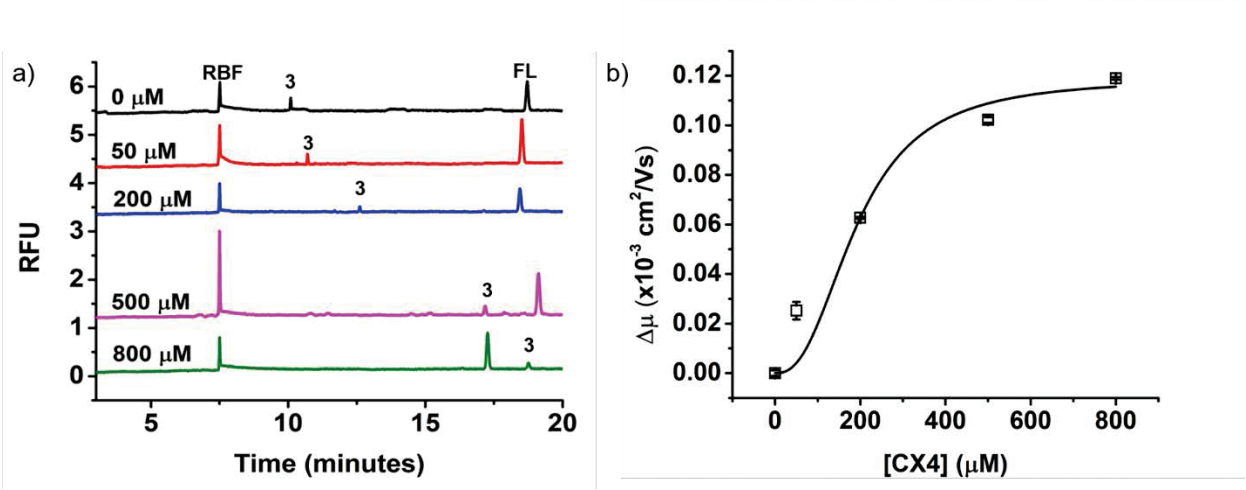

Figure S3. a) Mobility shift of the small dimethylated **3** guest as more **CX4** is added to the BGE (20 mM sodium phosphate buffer, pH 7.4). RBF = 10 μM riboflavin, FL = 50 nM fluorescein, **[3]** = 50 nM. b) A plot of Δμ vs. [**CX4**] for guest **3**. Each data point consists of triplicate measurements.

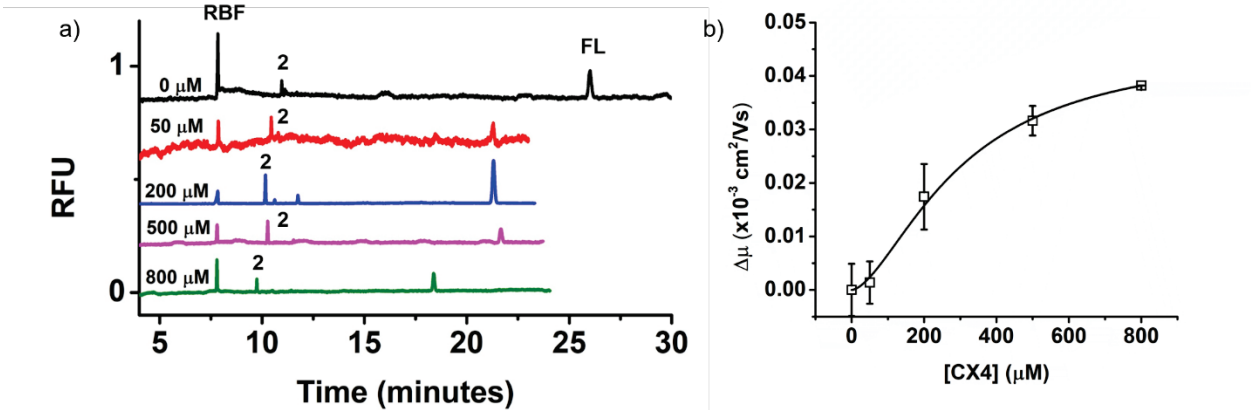

Figure S4. a) Mobility shift of the small monomethylated **2** guest as more **CX4** is added to the BGE (20 mM sodium phosphate buffer, pH 7.4). RBF = 10 μM riboflavin, FL = 50 nM fluorescein, [**2**] = 50 nM. b) A plot of Δμ vs. [**CX4**] for guest **2**. Each data point consists of triplicate measurements.

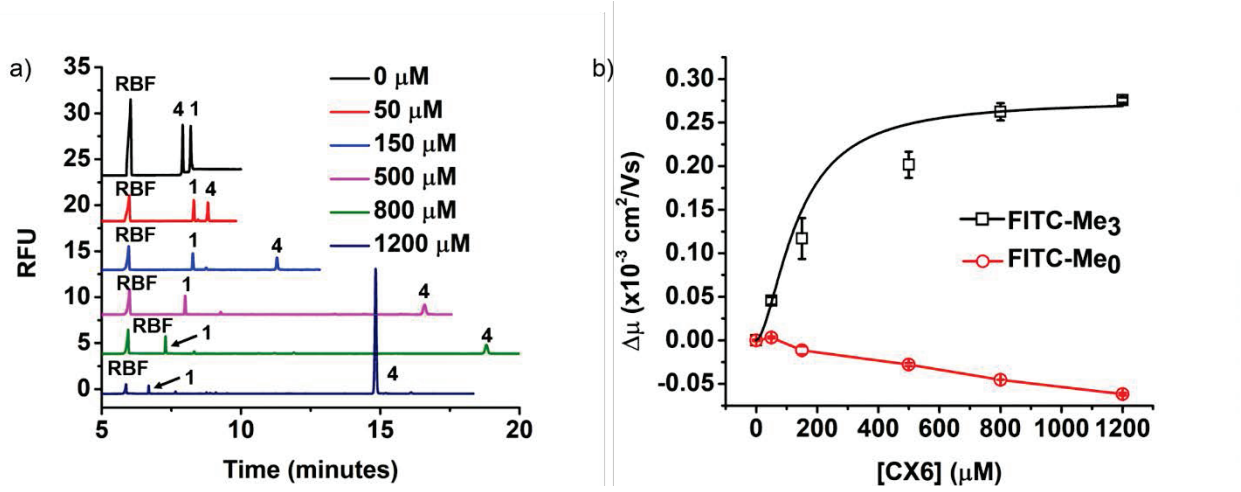

Figure S5. a) Mobility shift of the small trimethylated **4** guest as more **CX6** is added to the BGE (20 mM sodium phosphate buffer, pH 7.4). RBF = 10 μM riboflavin, [**1**] = 50 nM, [**4**] = 50 nM. b) A plot of Δμ vs. [**CX6**] for guests **4** and **1**. Each data point consists of triplicate measurements.

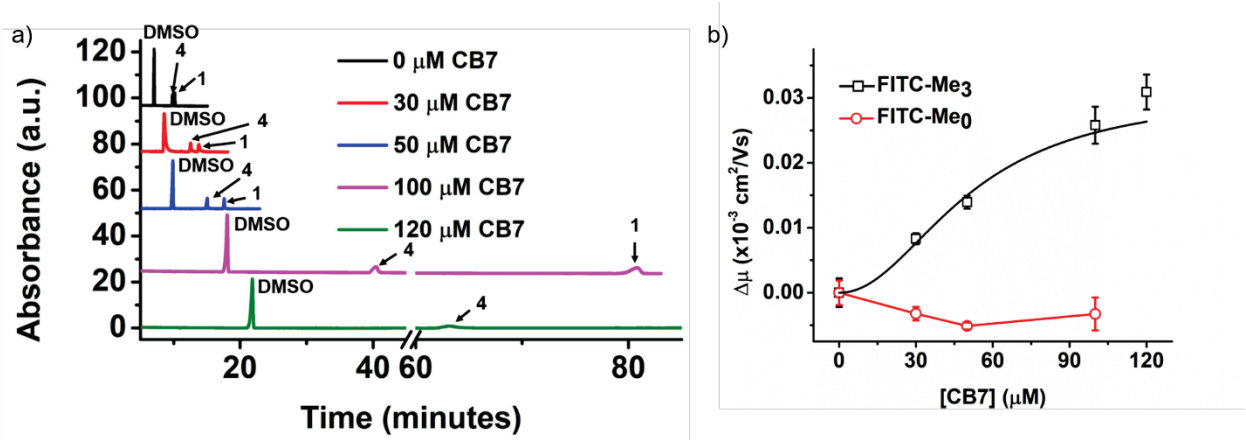

Figure S6. a) Mobility shift of the small trimethylated **4** guest as more **CB7** is added to the BGE (20 mM sodium phosphate buffer, pH 7.4). 0.1% DMSO, **[1]** = 50 nM, **[4]** = 50 nM. b) A plot of Δμ vs. [**CB7**] for guests **4** and **1**. Each data point consists of triplicate measurements.

Table S1. Summary of small guest curve fitting results for small molecular guests binding to the receptors.

Guest:Host	K_d	n	R^2	K_d
FITC-Me$_1$: CX4	299 ± 30 μM	1.6	0.998	Not detected
FITC-Me$_2$: CX4	192 ± 7 μM	2.5	0.989	157 μM
FITC-Me$_3$: CX4	100 ± 30 μM	1.7	0.995	125 μM
FITC-Me$_3$: CB7	51 ± 4 μM	2.0	0.949	Not measured
FITC-Me$_3$: CX6	135 ± 21 μM	1.7	0.998	Not measured

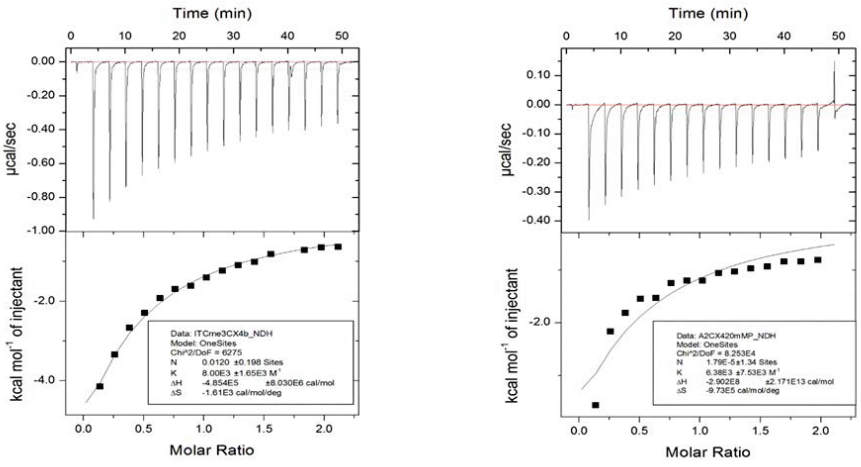

4. Analysis of Affinity between Methylated Peptides and Synthetic Hosts

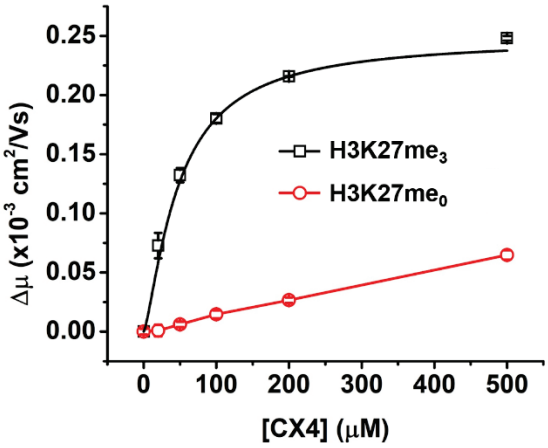

Figure S7. Plot of Δμ vs. [**CX4**] for labeled H3K27me$_3$ and H3K27me$_0$. Each data point consists of triplicate measurements.

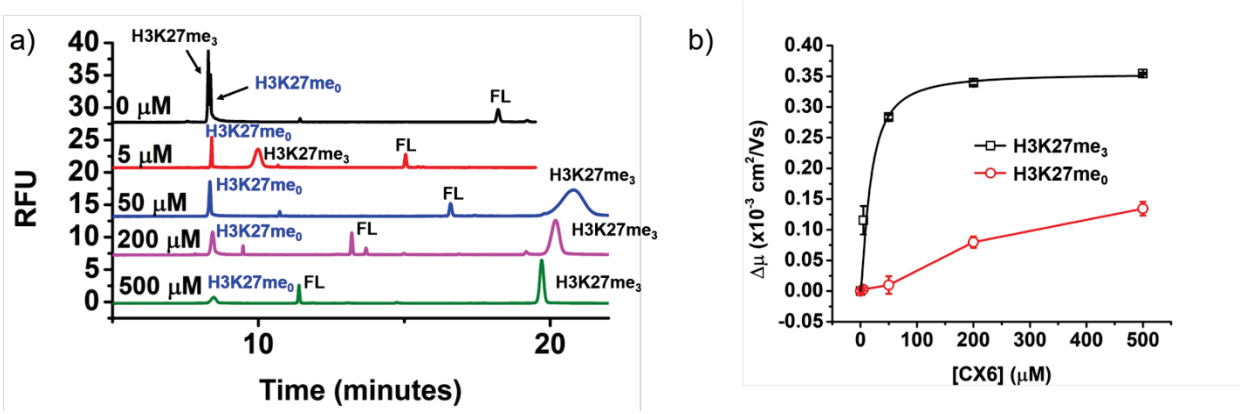

Figure S8. a) Mobility shift of labeled H3K27me$_3$ as more **CX6** is added to the BGE (20 mM sodium phosphate buffer, pH 7.4). [H3K27me$_3$] = [H3K27me$_0$] = 100 μM, FL = 50 nM fluorescein. b) A plot of Δμ vs. [**CX6**] for labeled H3K27me$_3$ and H3K27me$_0$. Each data point consists of triplicate measurements.

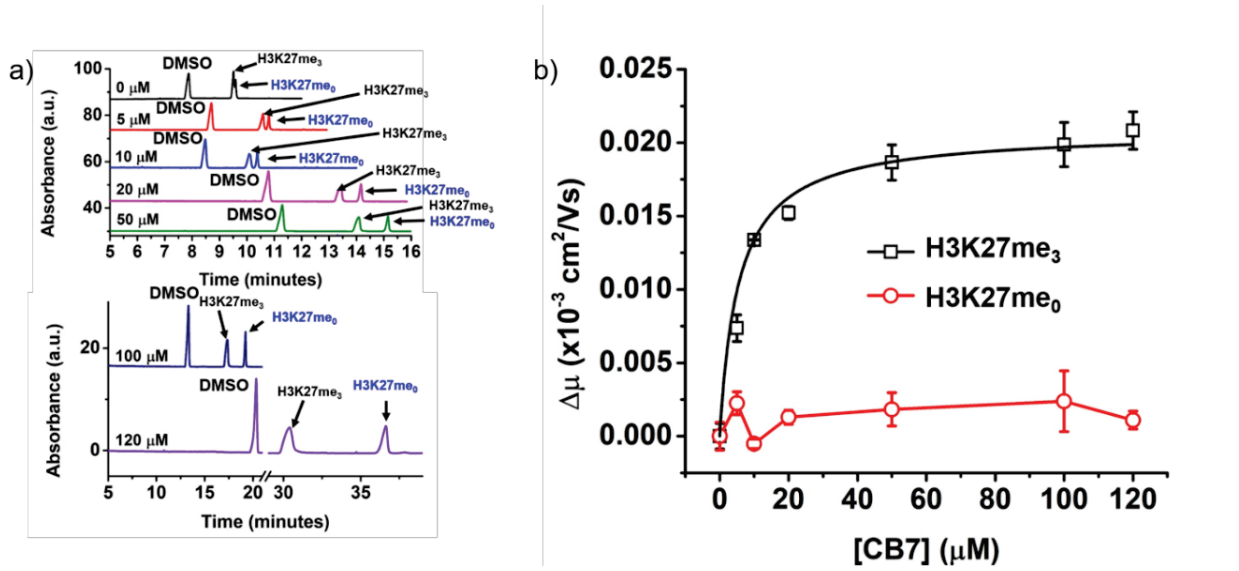

Figure S9. a) Mobility shift of labeled H3K27me$_3$ as more **CB7** is added to the BGE (20 mM sodium phosphate buffer, pH 7.4). 0.1% DMSO, [H3K27me$_3$] = [H3K27me$_0$] = 100 μM. b) A plot of Δμ vs. [**CX6**] for labeled H3K27me$_3$ and H3K27me$_0$. Each data point consists of triplicate measurements.

Table S2. Affinities between receptors and peptides measured by ITC compared to that obtained with CE.

Host	K_d, μM by CE	K_d, μM by ITC
CX4	48.0 ± 7.0	70.0
CX6	17.7 ± 4.2	11.7
CB7	5.5 ± 0.7	33.0

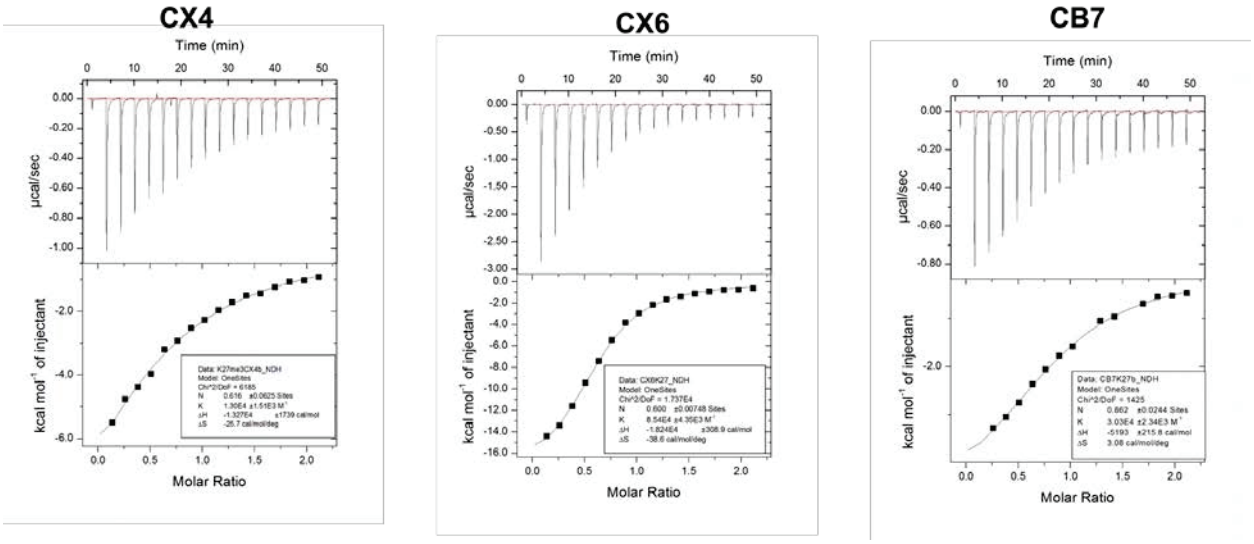

5. Summary of Resolution in Host-Assisted Capillary Electrophoresis

Table S3. Resolution of Various Guest and Peptide Peaks with Different Hosts in the Background Electrolyte

Guest/Peptide Pair	0 μM **CX4**	50 μM **CX4**	0 μM **CX6**	50 μM **CX6**	0 μM **CB7**	50 μM **CB7**
1/3, **2**/4	2.42		2.42		2.00	
2,**1**		1.25		0.85		5.62
1,**3**		3.69		1.97		2.85
3,**4**		2.41		4.98		4.97
$H3K27me_0$, $H3K27me_3$	0.15	4.40	0.15	26.47	0.63	2.65

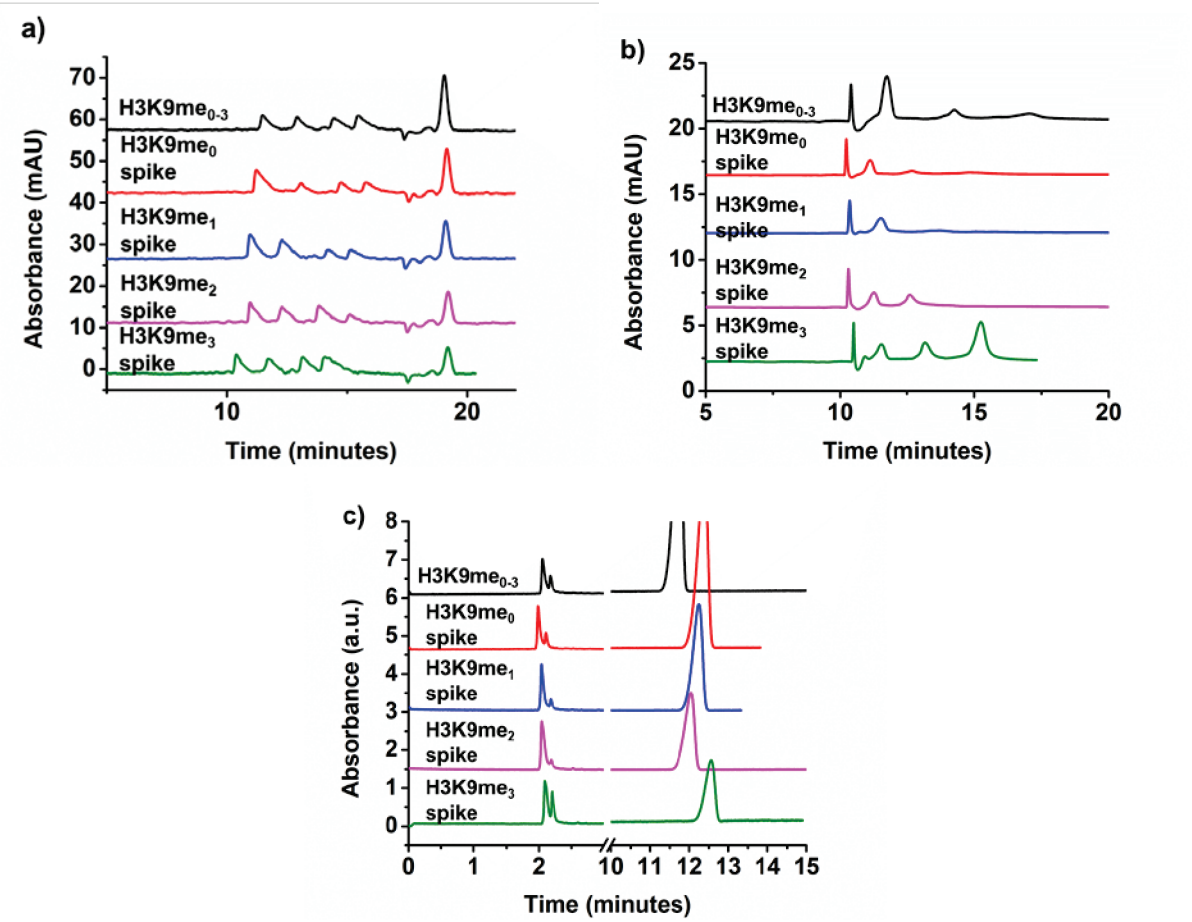

Figure S10. Spiked with standard peptides to confirm peak identity in peptide separation using a) CX4, b) CX6, and c) CB7.

6. Lysine Demethylase Assay

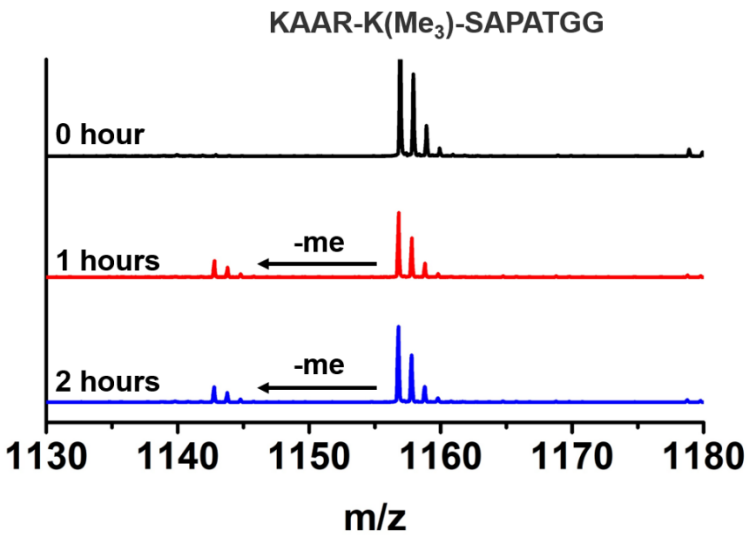

Figure S11. MALDI TOF/TOF spectra of substrate H3K27Me$_3$ and product H3K27Me$_2$ after demethylase enzyme reaction.

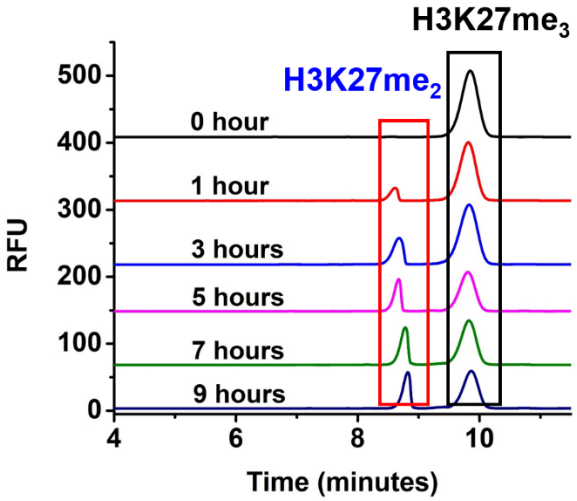

Figure S12. Separation of demethylated product H3K27(me$_2$) and H3K27(me$_3$) substrate after enzyme reaction for various times in the presence of 1 μM 2,4-PDCA inhibitor. Detection was carried out by the home-built laser induced fluorescence (LIF) system.

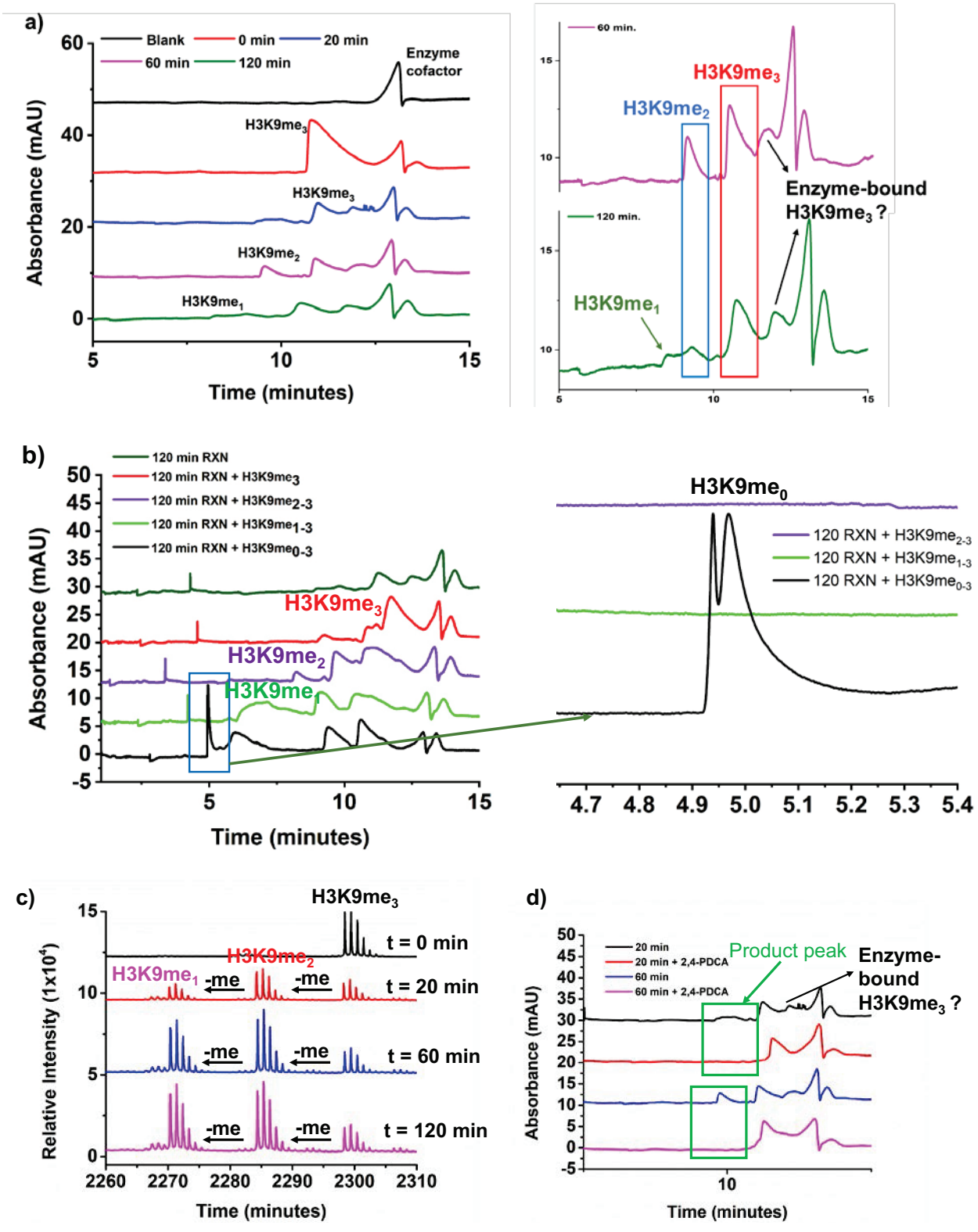

Figure S13. Analysis of the demethylation reaction of H3K9me$_3$ catalyzed by JMJD2E. a) Electropherograms collected at multiple reaction time points, with blank being the reaction

mixture without addition of enzyme and peptide substrate, and t = 0 min being the mixture containing the peptide substrate but not enzyme. b) Analysis of the reaction mixture at t = 120 min spiked with H3K9me$_3$, H3K9me$_2$, H3K9me$_1$, and H3K9me$_0$, consecutively for peak identification. The resolution got worse when more peptides were added to the sample due to column overloading. c) MALDI TOF/TOF spectra of substrate H3K9me$_3$ and products of H3K9me$_{1\text{-}2}$ after demethylase enzyme reaction. d) Analysis of reaction mixtures collected at 20 or 60 min. reaction duration with or without the presence of 1 μM 2,4-PDCA inhibitor. Separation was carried out in the Agilent CE system with UV detection at λ = 214 nm.